

## Generating Blending Surfaces with a Pseudo-Lévy Series Solution to Fourth Order Partial Differential Equations

L. H. You, Jian J. Zhang\*, and P. Comminos

Received November 12, 2002; revised June 8, 2003

Published online: October 30, 2003

© Springer-Verlag 2003

### Abstract

In our previous work, a more general fourth order partial differential equation (PDE) with three vector-valued parameters was introduced. This equation is able to generate a superset of the blending surfaces of those produced by other existing fourth order PDEs found in the literature. Since it is usually more difficult to solve PDEs analytically than numerically, many references are only concerned with numerical solutions, which unfortunately are often inefficient. In this paper, we have developed a fast and accurate resolution method, the pseudo-Lévy series method. Due to its analytical nature, the comparison with other existing methods indicates that the developed method can generate blending surfaces almost as quickly and accurately as the closed form resolution method, and has higher computational accuracy and efficiency than existing Fourier series and pseudo-spectral methods as well as other numerical methods. In addition, it can be used to solve complex surface blending problems which cannot be tackled by the closed form resolution method. To demonstrate the potential of this new method we have applied it to various surface blending problems, including the generation of the blending surface between parametric primary surfaces, general second and higher degree surfaces, and surfaces defined by explicit equations.

*AMS subject classification:* 35A20, 35A30, 35C10

*Key words:* Fast and accurate surface blending, fourth order partial differential equation, pseudo-Lévy series solution.

### 1. Introduction

Surface blending is a geometric modelling technique commonly used in computer aided design (CAD) to smoothly connect regular surfaces, such as second and higher degree surfaces. However, with the increasing demand of visual realism in computer graphics applications, such as computer animation, blends capable of handling both regular and free form surfaces are also often required. Such demands present the researchers of geometric modelling with an undeniable challenge. In order to develop powerful surface blending methods, we need to resolve two important issues. The first issue is the ability to blend various primary surfaces. The second issue relates to the computational efficiency and reliability of the method. It is frustrating to have to wait for a long while for a result in a design process.

---

\* Corresponding author

The generation of a blending surface by solving a partial differential equation is a powerful technique with which we can produce a smooth transition between two or more surfaces. Bloor et al [1] introduced a biharmonic-like fourth order PDE with one vector-valued parameter to solve some simple blending problems. In order to expand its applicability, various numerical PDE resolution methods were suggested. Using B-splines to represent the blending surfaces, a collocation method was developed [2] for the determination of the unknown parameters of the B-spline functions. This method was used to generate the blending surfaces between a cylinder and an inclined plane, and between two intersecting cylinders. Cheng et al. proposed a finite difference method to solve their fourth order PDE and produced the blending surfaces between two cylinders, and between a cone and a cylinder [3]. You and Zhang discussed the finite difference representation of surfaces based on a sixth order PDE [4]. Brown et al. investigated a B-spline finite element method, examined its effect on the accuracy of the solution with respect to element meshes of different sizes and differing degrees of B-spline surfaces, and generated a blending surface between a cylinder and an inclined plane [5, 6]. Li and Chang developed a boundary penalty finite element method for blending surfaces [7, 8, 9]. By combining a fourth order PDE with an equation of motion, Du and Qin developed a dynamic finite difference method for surface modelling [10, 11]. This method was further extended to PDE solid modelling [12]. Using more accurate PDEs developed from the dynamics of flat plates in bending, You et al. also proposed a dynamic finite difference method for the dynamic simulation of cloth [13]. In addition to the above numerical methods, Bloor et al. introduced a Fourier series method respectively for fourth order PDEs [14] and sixth order PDEs [15], a pseudo-spectral method [16] and a perturbation method [17] to perform surface generation and blending.

It is well known that the numerical methods such as the finite element method and finite difference method must solve a set of linear algebraic equations involving a large number of unknowns. These methods are computationally inefficient and thus often inappropriate in applications where interactive performance is required. The Fourier series method and the pseudo-spectral method, as will be seen later in this paper, are inaccurate. Although closed form solutions of PDEs have the highest computational efficiency and accuracy, since their determination is much more difficult than numerical solutions, only a few blending problems are solved in existing references. Such problems are referred to as periodic boundary conditions by Bloor et al. [16, 18].

In our previous work, we have proposed a more general fourth order PDE [19]. This equation has three vector-valued shape parameters and covers all forms of other existing fourth order PDEs used for surface blending. It therefore allows the designer to generate blending surfaces with a greater variety of shapes. We have also discussed the efficacy and efficiency of surface generation using various orders of PDEs [20], and surface blending using a closed form solution to a sixth order PDE [21]. In addition, we also proposed a new single-patch surface to represent tool shapes for hot metal forming [22]. In order to apply our fourth order PDE to various blending and surface representation problems, we will develop in this

paper a fast and accurate solution. Then we will compare this solution with a closed form solution, a Fourier series solution as well as a pseudo-spectral solution. To demonstrate the applications of the proposed solution in various blending problems, we will examine three blending problems. First, we will blend two primary surfaces expressed in parametric equations. Then, we will generate the blending surface between the second and higher degree general surfaces, which occur frequently in nature, science and engineering. Finally, we will generate the blending surfaces between two primary surfaces expressed in an explicit form.

### 2. The Pseudo-Lévy Series Solution of a PDE

In our previous work, we have reported that the vector-valued parameters of a fourth order PDE can exert a great influence on the shape of a blending surface and can be used as user handles to sculpture the shape of a blending surface. Due to this, we have introduced additional vector-valued parameters, known as the shape parameters, and proposed a more general fourth order PDE which has the form:

$$\left( \mathbf{b} \frac{\partial^4}{\partial u^4} + \mathbf{c} \frac{\partial^4}{\partial u^2 \partial v^2} + \mathbf{d} \frac{\partial^4}{\partial v^4} \right) \mathbf{X}(u, v) = \mathbf{f}(u, v) \tag{1}$$

where  $u$  and  $v$  are parametric variables,  $X = [x \ y \ z]^T$  is a vector-valued position function,  $\mathbf{b} = [b_x \ b_y \ b_z]^T$ ,  $\mathbf{c} = [c_x \ c_y \ c_z]^T$  and  $\mathbf{d} = [d_x \ d_y \ d_x]^T$  are vector-valued shape parameters, and  $\mathbf{f}(u, v) = [f_x(u, v) \ f_y(u, v) \ f_z(u, v)]^T$  is a vector-valued force function.

Eq. (1) is a general form of a fourth order PDE and includes all the forms of other existing fourth order PDEs used in surface blending.

To solve blending problems using a method based on the above PDE, we need to solve Eq. (1) subjected to the boundary conditions on the trimlines of the primary surfaces. These boundary conditions can be written as:

$$\begin{aligned} u = 0 \quad \mathbf{X} &= \mathbf{G}_1(v) & \frac{\partial \mathbf{X}}{\partial u} &= \mathbf{G}_2(v) \\ u = 1 \quad \mathbf{X} &= \mathbf{G}_3(v) & \frac{\partial \mathbf{X}}{\partial u} &= \mathbf{G}_4(v) \end{aligned} \tag{2}$$

where  $\mathbf{G}_i(v) = [G_{ix}(v) \ G_{iy}(v) \ G_{iz}(v)]^T$  ( $i = 1, 2, 3, 4$ ) are the continuity conditions of the position function  $X$  and its first partial derivatives on the trimlines  $u = 0$  and  $u = 1$ .

Eq. (1) under the boundary conditions (2) can be solved with various numerical methods such as the finite element method [6] and the finite difference method [3]. In order to meet the requirement for high computational efficiency, we will develop a fast and accurate resolution method in this paper.

First, we decompose the boundary conditions into the following two sets. For the first set  $\bar{\mathbf{G}}_i(v)$  ( $i = 1, 2, 3, 4$ ), the closed form solution of Eq. (1) is obtainable. For

the second set  $\bar{\bar{\mathbf{G}}}_i(v)(i = 1, 2, 3, 4)$ , the closed form solution of Eq. (1) does not exist.

$$\begin{aligned}
 u = 0 \quad \mathbf{X} &= \bar{\mathbf{G}}_1(v) + \bar{\bar{\mathbf{G}}}_1(v) & \frac{\partial \mathbf{X}}{\partial u} &= \bar{\mathbf{G}}_2(v) + \bar{\bar{\mathbf{G}}}_2(v) \\
 u = 1 \quad \mathbf{X} &= \bar{\mathbf{G}}_3(v) + \bar{\bar{\mathbf{G}}}_3(v) & \frac{\partial \mathbf{X}}{\partial u} &= \bar{\mathbf{G}}_4(v) + \bar{\bar{\mathbf{G}}}_4(v)
 \end{aligned}
 \tag{3}$$

Accordingly, we assume that the solution of Eq. (1) consists of two parts  $\mathbf{X} = \bar{\mathbf{X}} + \bar{\bar{\mathbf{X}}}$  where  $\bar{\mathbf{X}}$  is the closed form solution and  $\bar{\bar{\mathbf{X}}}$  is the non-closed form solution. Then we decompose the second set  $\bar{\bar{\mathbf{G}}}_i(v)(i = 1, 2, 3, 4)$  into a number of linearly independent basis functions which consist of elementary functions and their combinations in a non-polynomial form, i.e.,  $\bar{\bar{\mathbf{G}}}_i(v) = \sum_{j=1}^J \mathbf{a}_{ij} \mathbf{g}_j(v)(i = 1, 2, 3, 4)$ .

After the above treatment, the resolution of Eq. (1) under the boundary conditions (2) can be transformed into the task of finding the solutions of the following two sets of equations:

$$\begin{aligned}
 &\left( \mathbf{b} \frac{\partial^4}{\partial u^4} + \mathbf{c} \frac{\partial^4}{\partial u^2 \partial v^2} + \mathbf{d} \frac{\partial^4}{\partial v^4} \right) \bar{\mathbf{X}}(u, v) = \mathbf{0} \\
 u = 0 \quad \bar{\mathbf{X}} &= \bar{\mathbf{G}}_1(v) & \frac{\partial \bar{\mathbf{X}}}{\partial u} &= \bar{\mathbf{G}}_2(v) \\
 u = 1 \quad \bar{\mathbf{X}} &= \bar{\mathbf{G}}_3(v) & \frac{\partial \bar{\mathbf{X}}}{\partial u} &= \bar{\mathbf{G}}_4(v)
 \end{aligned}
 \tag{4}$$

and

$$\begin{aligned}
 &\left( \mathbf{b} \frac{\partial^4}{\partial u^4} + \mathbf{c} \frac{\partial^4}{\partial u^2 \partial v^2} + \mathbf{d} \frac{\partial^4}{\partial v^4} \right) \bar{\bar{\mathbf{X}}}(u, v) = \mathbf{f}(u, v) \\
 u = 0 \quad \bar{\bar{\mathbf{X}}} &= \sum_{j=1}^J \mathbf{a}_{1j} \mathbf{g}_j(v) & \frac{\partial \bar{\bar{\mathbf{X}}}}{\partial u} &= \sum_{j=1}^J \mathbf{a}_{2j} \mathbf{g}_j(v) \\
 u = 1 \quad \bar{\bar{\mathbf{X}}} &= \sum_{j=1}^J \mathbf{a}_{3j} \mathbf{g}_j(v) & \frac{\partial \bar{\bar{\mathbf{X}}}}{\partial u} &= \sum_{j=1}^J \mathbf{a}_{4j} \mathbf{g}_j(v)
 \end{aligned}
 \tag{5}$$

For Eq. (4), the resolution method can be found in our previous work [19]. Thus, here we only discuss the resolution method for Eq. (5).

The PDE in Eq. (5) is similar to the governing PDE of a flat plate subject to a uniformly distributed lateral load [23, 24]. For a simply supported flat plate under such a load, the Lévy series solution is very popular in mechanics. However, the boundary conditions of Eq. (5) are different to those of a simply supported flat plate. Therefore, the Lévy series solution has to be modified to meet the boundary conditions of Eq. (5). The modified solution is constructed by combining the two parts, where the first part satisfies the boundary conditions of Eq. (5) exactly and the second part has no influence on these boundary conditions, i.e.,

$$\begin{aligned} \bar{\mathbf{X}} = & \sum_{j=1}^J (\mathbf{p}_{1j} \sin \pi u + \mathbf{p}_{2j} u \sin \pi u + \mathbf{p}_{3j} \cos \pi u + \mathbf{p}_{4j} u \cos \pi u) \mathbf{g}_j(v) \\ & + \sin^2 \pi u \sum_{m=1}^M \xi_m(u) \sin mv \end{aligned} \tag{6}$$

where

$$\xi_m(u) = \mathbf{A}_m c h m \pi u + \mathbf{B}_m u s h m \pi u + \mathbf{C}_m s h m \pi u + \mathbf{D}_m u c h m \pi u \tag{7}$$

Substituting Eq. (6) into the boundary conditions of Eq. (5), the unknown constants  $\mathbf{p}_{ij}(i = 1, 2, 3, 4; j = 1, 2, \dots, J)$  in Eq. (6) are determined as:

$$\begin{aligned} \mathbf{p}_{1j} &= \frac{(\mathbf{a}_{1j} + \mathbf{a}_{2j} + \mathbf{a}_{3j})}{\pi} \\ \mathbf{p}_{2j} &= -\frac{(\mathbf{a}_{2j} + \mathbf{a}_{4j})}{\pi} \\ \mathbf{p}_{3j} &= \mathbf{a}_{1j} \\ \mathbf{p}_{4j} &= -(\mathbf{a}_{1j} + \mathbf{a}_{3j}) \end{aligned} \tag{8}$$

Then substituting Eq. (8) back into Eq. (6) and substituting Eq. (6) into the PDE of Eq. (5), since the solution (6) is an approximate solution, we obtain the following residual function:

$$\begin{aligned} \mathbf{R}(u, v) = & \sum_{m=1}^M [\mathbf{A}_m \mathbf{K}_{1m}(u, v) + \mathbf{B}_m \mathbf{K}_{2m}(u, v) + \mathbf{C}_m \mathbf{K}_{3m}(u, v) \\ & + \mathbf{D}_m \mathbf{K}_{4m}(u, v)] - \mathbf{E}(u, v) \end{aligned} \tag{9}$$

For brevity, the concrete forms of  $\mathbf{K}_{1m}(u, v)$ ,  $\mathbf{K}_{2m}(u, v)$ ,  $\mathbf{K}_{3m}(u, v)$ ,  $\mathbf{K}_{4m}(u, v)$  and  $\mathbf{E}(u, v)$  are not given here. The unknown constants in the above equations are  $\mathbf{A}_m, \mathbf{B}_m, \mathbf{C}_m, \mathbf{D}_m(m = 1, 2, \dots, M)$ . Within the resolution region, uniformly choosing  $N \geq 4M$  collocation points, calculating the residual values of the residual function  $\mathbf{R}(u, v)$  at these collocation points, and following the mathematical derivation given by You et al. [25], we obtain the following linear algebraic equations:

$$\mathbf{K}^T \mathbf{K} \delta = \mathbf{K}^T \mathbf{F} \tag{10}$$

Solving equation (10) for the unknown constants  $\mathbf{A}_m, \mathbf{B}_m, \mathbf{C}_m, \mathbf{D}_m(m = 1, 2, \dots, M)$  and substituting them back into Eq. (7), the solution to Eq. (5) is obtained. Superimposing the closed form solution of Eq. (4) and the solution of Eq. (5), the general solution of the PDE (1) subject to the boundary conditions (2) is obtained. We call this the pseudo-Lévy series solution.

### 3. Comparison of Different Approaches

In order to demonstrate the high computational accuracy, efficiency and efficacy of the developed method in surface modelling, in this section we compare it with the closed form resolution method, the Fourier series method [14] and the pseudo-spectral method [16]. The latter two are faster than other numerical methods.

The closed form solution is an accurate solution. To achieve such a solution, we use the following boundary conditions which define a blending surface between a plane and an ellipse, for which the closed form solution of Eq. (1) exists.

$$\begin{aligned}
 u = 0 \quad & x = 1 + 0.00005e^v & \frac{\partial x}{\partial u} &= 0 \\
 & y = 1 - \frac{v}{\pi} & \frac{\partial y}{\partial u} &= 0 \\
 & z = 1.5 & \frac{\partial z}{\partial u} &= -1.5 \\
 u = 1 \quad & x = -0.2 \cos v & \frac{\partial x}{\partial u} &= 0 \\
 & y = 0.5 \sin v & \frac{\partial y}{\partial u} &= 0 \\
 & z = 0 & \frac{\partial z}{\partial u} &= -1.5
 \end{aligned} \tag{11}$$

Using the resolution method given by [19] and without considering the force function, the closed form solution of the PDE (1) subjected to the boundary conditions (11) has the form:

$$\begin{aligned}
 x &= \sum_{n=0}^3 c_{xi}u^i + R_{x1}(u) \cos v + R_{x2}(u)e^v \\
 y &= \sum_{n=0}^3 (c_{y1i} + c_{y2i}v)u^i + R_{y1}(u) \sin v \\
 z &= \sum_{n=0}^3 c_{zi}u^i
 \end{aligned} \tag{12}$$

where the concrete forms of  $R_{x1}(u)$ ,  $R_{x2}(u)$  and  $R_{y1}(u)$  can be determined by substituting the first two components  $x$  and  $y$  of Eq. (12) into the PDE (1) and all the unknown constants can be determined by substituting Eq. (12) into the boundary conditions (11).

Using the shape parameters  $b_x = b_y = b_z = 1$ ,  $c_x = c_y = c_z = 50$  and  $d_x = d_y = d_z = 625$ , we have generated the blending surfaces shown in Fig. 1a.

In order to investigate the computational efficiency and accuracy of our method, we use it to determine the solution of the PDE (1) corresponding to the term containing  $e^v$  in the boundary conditions (11). According to Eq. (6), the solution can be written as:

$$\begin{aligned}
 \bar{\mathbf{X}} &= (\mathbf{p}_{11} \sin \pi u + \mathbf{p}_{21}u \sin \pi u + \mathbf{p}_{31} \cos \pi u + \mathbf{p}_{41}u \cos \pi u)e^v \\
 &+ \sin^2 \pi u \sum_{m=1}^M \xi_m(u) \sin mv
 \end{aligned} \tag{13}$$

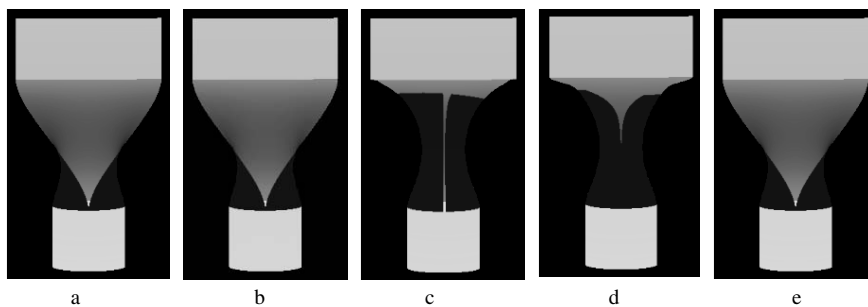


Fig. 1. Comparison between different blending methods

Following the developed method, we can obtain the set of linear algebraic equations (10) whose resolution determines all the unknown constants in Eq. (13). Then superimposing the closed form solution and the solution (13), we obtain a general solution. With the same shape parameters, uniformly choosing collocation points within the resolution region, and setting the terms of the Lévy series to  $M = 4$ , we have created the blending surfaces depicted in Fig. 1b. Clearly, there are no visible differences between Figs. 1a and 1b. This is a good indication of the accuracy of the developed method.

When using the Fourier series method, the terms containing  $v$  and  $e^v$  must first be expanded into the Fourier series. Then, the Fourier series solution of the PDE (1) subjected to the boundary conditions (11) can be obtained using the method given in [14]. Using the same shape parameters and taking the terms of the Fourier series to be 10, the generated blending surface is given in Fig. 1c.

It is apparent that the blending surface in Fig. 1c is quite different from that in Fig. 1a. On the upper boundary, between the upper primary surface and the blending surface, the Fourier series solution fails to give a reasonable approximation. As a consequence, the upper boundary conditions are not satisfied. At the two ends of the upper boundary curve, the values given by the Fourier series are the average values of these two end points, which leads to discontinuities of the boundary curve at these two ends. As a result, a narrow gap appears all the way through to the bottom boundary in the figure.

In order to overcome the shortcomings of the Fourier series solution, a pseudo-spectral method was developed [16]. In this method, a remainder function is superimposed on the Fourier series solution. Then the unknown functions in the remainder function are determined by meeting the boundary conditions exactly. However, this introduces another problem, i.e., the PDE (1) cannot be satisfied after the addition of the remainder function. Fig. 1d shows the result of this method. There is a clear discrepancy between Fig. 1d and the accurate one in Fig. 1a.

In addition to its inaccuracy, the Fourier series solution requires a large number of Fourier series terms to approximate the accurate solution leading to a slow

resolution process. For the pseudo-spectral method, a tedious mathematical derivation must be carried out to obtain the explicit form of the unknown functions in the remainder function by exactly satisfying the boundary conditions. Otherwise, a large number of linear equations of the 4th order have to be solved to determine the unknowns of the remainder function at the points on the boundary curves which will be used to generate the blending surfaces. This slows down the resolution process significantly.

The closed form solution is the most efficient. For the blending surface given in Fig. 1a, it took less than  $10^{-6}$  of a second on an 800 MHz PC to determine all the unknowns. For the blending surface shown in Fig. 1b, the pseudo-Lévy series method also took less than  $10^{-6}$  of a second for the determination of all the unknowns. This shows that the developed pseudo-Lévy series method can generate blending surfaces almost as fast as the closed form resolution method, and faster than the Fourier series and the pseudo-spectral methods.

#### 4. Blending Surfaces Expressed in a Parametric Form

Primary surfaces expressed in a parametric form are widely used in computer aided design and computer graphics. Usually their boundary conditions consist of constants, parametric variable  $v$  and its power functions, sine, cosine, and exponential functions. In this section, we will present some examples to show the application of the developed approach in such blending problems.

*The blending Surface Between a Primary Surface With Trimlines Consisting of Sine and Cosine Functions and a Plane Containing a Pre-specified Ellipse*

Given that the solving region is over  $\Omega : \{0 \leq u \leq 1; 0 \leq v \leq 2\pi\}$ , the primary surface consisting of sine and cosine functions can be described by the following parametric equations:

$$\begin{aligned} x &= (1 + \xi u^2)(R_0 \cos v + R_1 \cos kv) \\ y &= (1 + \xi u^2)(R_0 \sin v + R_1 \sin kv) \\ z &= h_0 + h_1 u \end{aligned} \tag{14}$$

and the plane is assumed to have the form of:

$$\begin{aligned} x &= au \cos v \\ y &= bu \sin v \\ z &= 0 \end{aligned} \tag{15}$$

Taking the trimlines to be at  $u = u_0$  on the primary surface (14) and at  $u = u_1$  on the plane (15), the boundary conditions on these trimlines can be written as:



$$\begin{aligned}
 u = 0 \quad x &= (1 + \xi u_0^2)(R_0 \cos v + R_1 \cos kv) & \frac{\partial x}{\partial u} &= 2\xi' u_0(R_0 \cos v + R_1 \cos kv) \\
 y &= (1 + \xi u_0^2)(R_0 \sin v + R_1 \sin kv) & \frac{\partial y}{\partial u} &= 2\xi' u_0(R_0 \sin v + R_1 \sin kv) \\
 z &= h_0 + h_1 u_0 & \frac{\partial z}{\partial u} &= h'_1 \\
 u = 1 \quad x &= a u_1 \cos v & \frac{\partial x}{\partial u} &= a' \cos v \\
 y &= b u_1 \sin v & \frac{\partial y}{\partial u} &= b' \sin v \\
 z &= 0 & \frac{\partial z}{\partial u} &= 0
 \end{aligned} \tag{16}$$

Using the developed pseudo-Lévy series method, the blending surface is produced as shown in Fig. 2. The relative parameters used in this blending operation were taken to be:  $u_0 = R_1 = 0.1$ ,  $u_1 = 1$ ,  $R_0 = 0.9$ ,  $h_1 = h'_1 = 1.5$ ,  $h_0 = \xi = \xi' = 0.5$ ,  $a = a' = 1.6$ , and  $b = b' = 1.2$ .

*The Blending Surface Between Two Intersecting Planes  
with Two Non-Parallel Trimlines*

The blending surface between two intersecting planes frequently appears in mechanical components to simplify the manufacturing process or to reduce the stress concentration at the joint between the two planes. The boundary conditions for this blending operation can be written as:

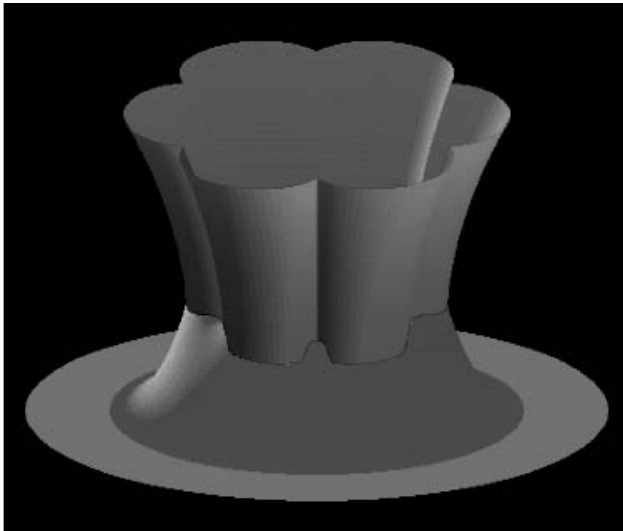


**Fig. 2.** The blending surface between a surface with the trimline consisting of trigonometric functions and a plane with a pre-specified ellipse

$$\begin{aligned}
 u = 0 \quad x = 0 \quad \frac{\partial x}{\partial u} = 0 \\
 \quad \quad y = h_0 + h_1 v \quad \frac{\partial y}{\partial u} = -(h_2 + h_3 v) \\
 \quad \quad z = pv \quad \frac{\partial z}{\partial u} = 0 \\
 u = 1 \quad x = s_0 + s_1 v \quad \frac{\partial x}{\partial u} = s_2 + s_3 v \\
 \quad \quad y = 0 \quad \frac{\partial y}{\partial u} = 0 \\
 \quad \quad z = pv \quad \frac{\partial z}{\partial u} = 0
 \end{aligned} \tag{17}$$

Setting parameters in Eq. (17) to be:  $h_0 = 0.9, h_1 = -0.4, h_2 = 1.1, h_3 = s_3 = 0.01, s_0 = 1, s_1 = -0.5, s_2 = 1.2$  and  $p = 2$ , we have generated the blending surface shown in Fig. 3a.

The above method also applies to the blending where the two trimlines meet at the intersection line of the two planes. To do this, the boundary conditions should be properly modified, i.e.,  $y = h_0 + h_1 v$ , is changed to  $y = h_1 v$  and  $x = s_0 + s_1 v$  is changed to  $x = s_1 v$ . The blending surface shown in Fig. 3b was generated by setting  $h_1 = 0.9, h_2 = 0.02, h_3 = 2.0, s_1 = 1.0, s_2 = 0.01, s_3 = 0.9$  and keeping the other parameters unchanged.

When using a cone to blend these two planes, the cross section of the cone is a regular closed curve such as a circle or an ellipse. On the other hand when using the method described in this paper to perform this blending operation, the generated blending surface can also be regarded as a part of a generalised cone whose cross section is an irregular closed curve. The circular and elliptic curves, of the former method, are only special cases of this irregular closed curve. Therefore, the later method is more flexible, as it can generate more varied blending surfaces.

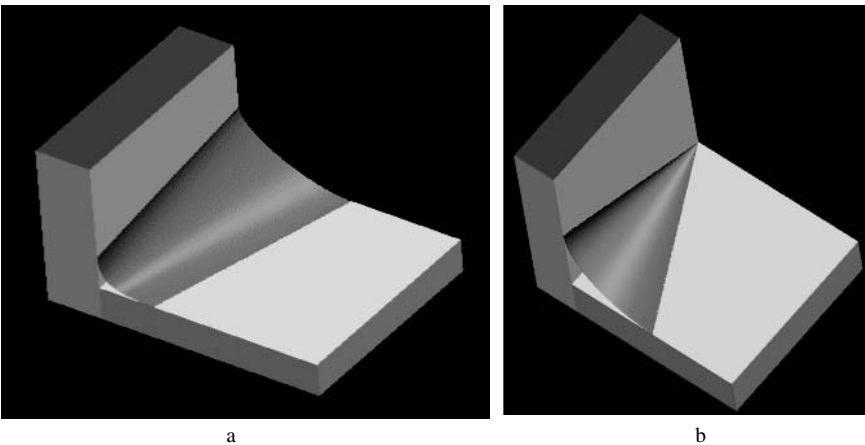


Fig. 3. The blending surface between two perpendicular planes with inclined trimlines

*The Blending Surface Between Two Intersecting Cylinders*

Compared to the closed form resolution method, the developed pseudo-Lévy series method is more powerful due to its ability to tackle complex surface blending problems. To demonstrate this point, we present as an example the blending surface between two intersecting cylinders. In the existing references of PDE-based surface blending, such problems could only be solved using numerical methods.

The boundary conditions for this surface blending problem are given as follows

$$\begin{aligned}
 u = 0 \quad & x = s \cos v & \frac{\partial x}{\partial u} &= 0 \\
 & y = s \sin v & \frac{\partial y}{\partial u} &= 0 \\
 & z = \sqrt{(r + k_1)^2 - s^2 \cos^2 v} & \frac{\partial z}{\partial u} &= \frac{r+k_1}{\sqrt{(r+k_1)^2 - s^2 \cos^2 v}} \\
 u = 1 \quad & x = (s + l_1) \cos v & \frac{\partial x}{\partial u} &= t(s + l_1) \cos v \\
 & y = (s + l_1) \sin v & \frac{\partial y}{\partial u} &= t(s + l_1) \sin v \\
 & z = \sqrt{r^2 - (s + l_1)^2 \cos^2 v} & \frac{\partial z}{\partial u} &= -t \frac{(s+l_1) \cos^2 v}{\sqrt{r^2 - (s+l_1)^2 \cos^2 v}}
 \end{aligned} \tag{18}$$

where  $s, r, k_1$  and  $l_1$  are the geometric parameters defining the two boundary curves, and  $t$  is the parameter controlling the first partial derivatives on the boundary curves.

Using the developed pseudo-Lévy series method, the PDE (1) under the boundary conditions for the  $x$  and  $y$  components of Eq. (18) has a closed form solution. However, it does not have a closed form solution subject to the boundary condition of the  $z$  component of Eq. (18). Our method is very useful in solving this class of problems. Rewriting the boundary conditions for the component of Eq. (18) in the form of Eq. (5), we can identify the linearly independent basis functions for the component, which are:

$$\begin{aligned}
 g_{1z}(v) &= \sqrt{(r+k_1)^2 - s^2 \cos^2 v} \\
 g_{2z}(v) &= \frac{1}{\sqrt{(r+k_1)^2 - s^2 \cos^2 v}} \\
 g_{3z}(v) &= \sqrt{r^2 - (s + l_1)^2 \cos^2 v} \\
 g_{4z}(v) &= \frac{\cos^2 v}{\sqrt{r^2 - (s + l_1)^2 \cos^2 v}}
 \end{aligned} \tag{19}$$

After the above treatment, the general solution of the PDE (1) for this blending surface problem can be expressed as:

$$\begin{aligned}
 x &= R_{x1}(u) \cos v \\
 y &= R_{y1}(u) \sin v
 \end{aligned}$$

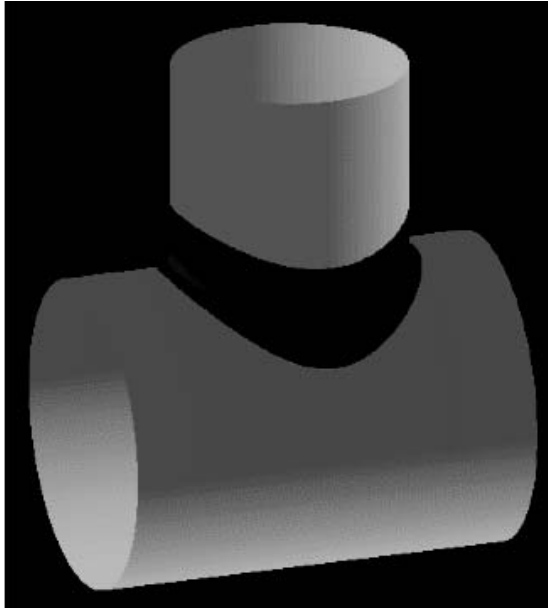


**Fig. 4.** The blending surface between two intersecting cylinders

$$\begin{aligned}
 z = & \sum_{j=1}^4 [p_{z1j} \sin \pi u + p_{z2j} u \sin \pi u + p_{z3j} \cos \pi u + p_{z4j} u \cos \pi u] g_{jz}(v) \\
 & + \sin^2 u \sum_{m=1}^M \xi_m(u) \sin mv
 \end{aligned}
 \tag{20}$$

Using our method, we can determine all the unknown constants in Eq. (20) and the generated blending surface is given in Fig. 4.

#### *Vertex Blending*

Above, we have discussed parametric blending between two primary surfaces. By modifying Eq. (6), our method can also be employed to blend three or four primary surfaces. Since the mathematical manipulation for this case is much more complex, it will not be discussed here. In Fig. 5, only the blending surface between three primary surfaces was depicted. Here the image on the left depicts the original cube, while the image on the right depicts the cube after one of its vertices has been blended and three of its edges have been filleted.

### **5. Blending General Surfaces of Second or Higher Degree**

General surfaces of the second or higher degree are among the most popular surfaces existing in engineering. These surfaces include: spheres, cylinders,

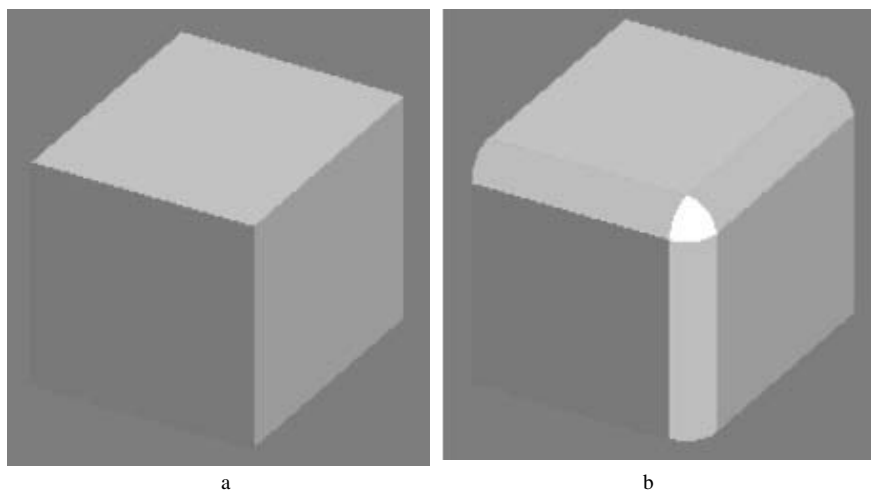


**Fig. 5.** Blending of a corner

ellipsoids, tori, hyperboloids of one sheet, hyperboloids of two sheets, elliptical paraboloids, and cones, etc. The mathematical formulations of such surfaces are generally given in an implicit form. However, these implicit equations can be transformed into parametric equations after suitable parameter substitution. Here, we will use an implicit mathematical representation for the primary surfaces and a parametric form of the boundary conditions on the trimlines.

*The Blending Surface Between an Elliptical Cone and an Ellipsoid*

The implicit equations of an elliptical cone and an ellipsoid are respectively given by:

$$\frac{x^2}{a^2} + \frac{y^2}{b^2} - \frac{z^2}{h^2} = 0$$

and

$$\frac{x^2}{R^2} + \frac{y^2}{R^2} + \frac{z^2}{s^2} - 1 = 0$$

Taking the trimlines on the elliptical cone to be  $z = h$  and on the ellipsoid to be  $z = \frac{\sqrt{2}}{2}s$ , the boundary conditions in a parametric form for this blending surface can be written as:

$$\begin{aligned}
 u = 0 \quad & x = \frac{\sqrt{2}}{2} R \cos v & \frac{\partial x}{\partial u} &= -\frac{\sqrt{2}}{2} R' \cos v \\
 & y = \frac{\sqrt{2}}{2} R \sin v & \frac{\partial y}{\partial u} &= -\frac{\sqrt{2}}{2} R' \sin v \\
 & z = \frac{\sqrt{2}}{2} s & \frac{\partial z}{\partial u} &= \frac{\sqrt{2}}{2} s' \\
 u = 1 \quad & x = a \cos v & \frac{\partial x}{\partial u} &= a' \cos v \\
 & y = b \sin v & \frac{\partial y}{\partial u} &= b' \sin v \\
 & z = h & \frac{\partial z}{\partial u} &= h'
 \end{aligned}
 \tag{21}$$

The blending surface obtained from the above boundary conditions is shown in Fig. 6.

*The Blending Surface Between a Hyperboloid of One Sheet and a Circular torus*

The implicit equations of a hyperboloid of one sheet and a circular torus are respectively given by:

$$\frac{x^2}{a^2} + \frac{y^2}{b^2} - \frac{(z - h_0)^2}{h^2} - 1 = 0$$

and

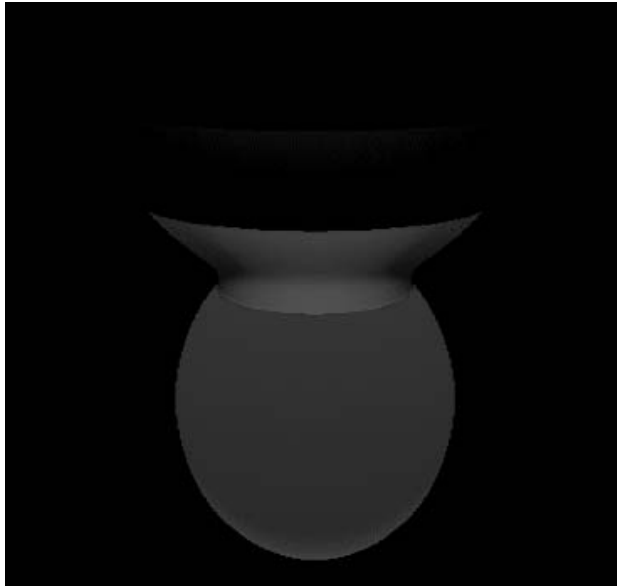


**Fig. 6.** The blending surface between an elliptical cone and an ellipsoid

$$(x^2 + y^2 + z^2 - A^2 + R^2)^2 - 4R^2(x^2 + y^2) = 0$$

Taking the trimlines on the hyperboloid of one sheet to be  $u = u_0$  and on the torus to be  $u = u_1$ , the boundary conditions for this blending surface can be written as the following parametric form:

$$\begin{aligned}
 u = 0 \quad & x = a \cosh u_0 \cos v & \frac{\partial x}{\partial u} &= a' \sinh u_0 \cos v \\
 & y = b \cosh u_0 \sin v & \frac{\partial y}{\partial u} &= b' \sinh u_0 \sin v \\
 & z = h_0 + h \sinh u_0 & \frac{\partial z}{\partial u} &= h' \cosh u_0 \\
 u = 1 \quad & x = (R + A \cos u_1) \cos v & \frac{\partial x}{\partial u} &= -A' \sin u_1 \cos v \\
 & y = (R + A \cos u_1) \sin v & \frac{\partial y}{\partial u} &= -A' \sin u_1 \sin v \\
 & z = A \sin u_1 & \frac{\partial z}{\partial u} &= A' \cos u_1
 \end{aligned} \tag{22}$$

The blending surface obtained from the above boundary conditions is shown in Fig. 7.

### 6. Blending Surfaces Expressed in Explicit form

The developed pseudo-Lévy series solution of Eq. (1) can also be used to solve surface blending problems between two primary surfaces expressed in an explicit form. Next, we will examine two different types of explicit functions used to



Fig. 7. The blending surface between a circular torus and a hyperboloid of one sheet

represent the primary surfaces and we will show how the blending surfaces can be generated in each case.

*The Blending Surface Between a Cylinder and a Plane Containing a Specified Straight Line or Curve*

First, we discuss the blending between a cylinder and a plane containing a straight line. The explicit equation of the cylinder is assumed to be:

$$y = \sum_0^m a_i x^i \tag{23}$$

We start by introducing a new variable  $v$  and assuming that the following relationship holds between the new variable  $x$  and the original variable

$$x = r \cos v \tag{24}$$

Then, substituting Eq. (24) into Eq. (23) and making use of the relationship:

$$\begin{aligned} \cos^i v &= \cos iv + \frac{i(i-1)}{2!} \cos^{i-2} v \sin^2 v - \frac{i(i-1)(i-2)(i-3)}{4!} \cos^{i-4} v \sin^4 v \\ &+ \frac{i(i-1)(i-2)(i-3)(i-4)(i-5)}{6!} \cos^{i-6} v \sin^6 v - \dots \end{aligned} \tag{25}$$

$$\sin^{2i} v = (1 - \cos^2 v)^i$$

the explicit equation (23) defining the primary surface can be transformed into the following parametric equation:

$$y = \sum_0^m b_i \cos iv \tag{26}$$

For example, taking  $m = 6$  in Eq. (23), the coefficients  $b_i (i = 0, 1, 2, \dots, 6)$  in Eq. (26) can be linked to the coefficients in Eq. (23) with the following relationships:

$$\begin{aligned} b_0 &= a_0 + \frac{1}{2} a_2 r^2 + \frac{3}{8} a_4 r^4 + \frac{5}{16} a_6 r^6 \\ b_1 &= a_1 r + \frac{3}{4} a_3 r^3 + \frac{5}{8} a_5 r^5 \\ b_2 &= \frac{1}{2} a_2 r^2 + \frac{1}{2} a_4 r^4 + \frac{15}{32} a_6 r^6 \\ b_3 &= \frac{1}{4} a_3 r^3 + \frac{5}{16} a_5 r^5 \\ b_4 &= \frac{1}{8} a_4 r^4 + \frac{3}{16} a_6 r^6 \\ b_5 &= \frac{1}{16} a_5 r^5 \\ b_6 &= \frac{1}{32} a_6 r^6 \end{aligned} \tag{27}$$



The boundary conditions for this blending surface are:

$$\begin{aligned}
 u = 0 \quad & x = r \cos v & \frac{\partial x}{\partial u} &= 0 \\
 & y = \sum_{i=0}^6 b_i \cos iv & \frac{\partial y}{\partial u} &= 0 \\
 & z = hu_0 & \frac{\partial z}{\partial u} &= h' \\
 u = 1 \quad & x = p_0 - p_1v & \frac{\partial x}{\partial u} &= 0 \\
 & y = s_0 + s_1(1 - u_1) & \frac{\partial y}{\partial u} &= -s'_1 \\
 & z = 0 & \frac{\partial z}{\partial u} &= 0
 \end{aligned} \tag{28}$$

Requiring  $0 \leq v \leq \frac{\pi}{2}$ , and setting the values of the coefficients in Eq. (23) to be  $a_0 = 0.35$ ,  $a_1 = 4.223$ ,  $a_2 = -12.924$ ,  $a_3 = 9.4799$ ,  $a_4 = -0.12972$ ,  $a_5 = -1.7385$ ,  $a_6 = 0.39685$ ,  $u_0 = 0.7$  and  $u_1 = 0.8$ , we obtain the blending surface shown in Fig. 8.

Next, we replace the straight trimline on the plane with a curve that changes the boundary conditions on  $u = 1$  of Eq. (28) to:

$$\begin{aligned}
 u = 1 \quad & x = e_0 - e_1v & \frac{\partial x}{\partial u} &= 0 \\
 & y = -(e_2 + e_3v^2)u_1 & \frac{\partial y}{\partial u} &= -(e'_2 + e'_3v^2) \\
 & z = 0 & \frac{\partial z}{\partial u} &= 0
 \end{aligned} \tag{29}$$

Setting  $u_1 = 0.9$  generates the blending surface shown in Fig. 9.

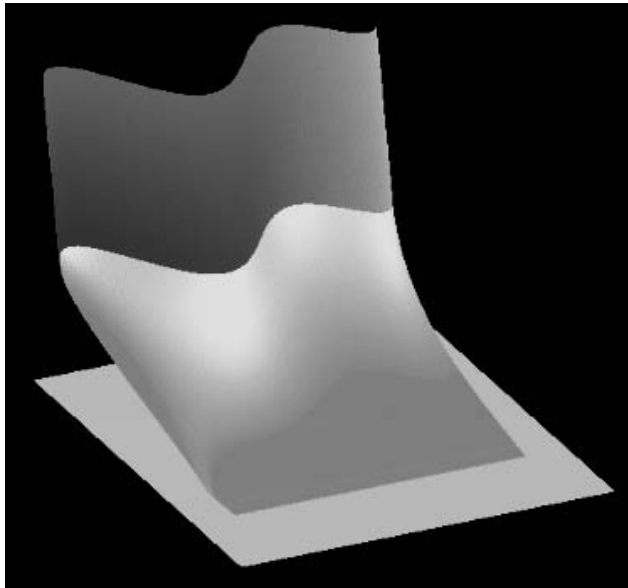


**Fig. 8.** The blending surface between a cylinder and a plane containing a pre-specified line

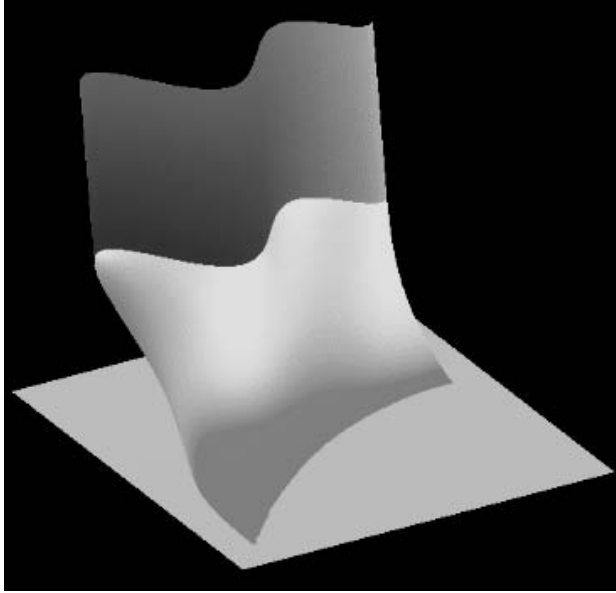


**Fig. 9.** The blending surface between a cylinder and a plane containing a pre-specified curve

*The Blending Surface Between a General Primary Surface and a Plane Containing a Specified Curve*

In the above example, we have discussed the blending surface between a cylinder surface expressed in an explicit form and a plane. Here we examine the blending surface between a general surface defined by the explicit function  $y = h(x, z)$  and a plane containing a specified curve. The form of the  $y$  co-ordinate is taken to be:

$$y = a_0z^5 \cos z + a_1xz^4 + a_2x^2 \sin z + a_3x^3 \cosh z + a_4x^4z + a_5x^5 \tag{30}$$

We apply the same substitution to the  $x$  coordinate as above and we introduce the relationship  $z = u$ . The specified curve on the plane is taken to be a quarter of a circle. The boundary conditions for this blending surface can be written as:

$$\begin{aligned}
 u = 0 \quad & x = r \cos v & \frac{\partial x}{\partial u} &= 0 \\
 & y = \sum_{i=0}^5 b_i \cos iv & \frac{\partial y}{\partial u} &= \sum_{i=0}^4 b'_i \cos iv \\
 & z = u_0 & \frac{\partial z}{\partial u} &= -1 \\
 u = 1 \quad & x = u_1(c - R \cos v) & \frac{\partial x}{\partial u} &= (c' - R' \cos v) \\
 & y = u_1(d - R \sin v) & \frac{\partial y}{\partial u} &= (d' - R' \sin v) \\
 & z = 0 & \frac{\partial z}{\partial u} &= 0
 \end{aligned} \tag{31}$$

where

$$\begin{aligned}
 b_0 &= a_0u_0^5 \cos u_0 + \frac{1}{2}a_2r^2 \sin u_0 + \frac{3}{8}a_4r^4u_0 \\
 b_1 &= a_1ru_0^4 + \frac{3}{4}a_3r^3 \cosh u_0 + \frac{5}{8}a_5r^5 \\
 b_2 &= \frac{1}{2}a_2r^2 \sin u_0 + \frac{1}{2}a_4r^4u_0 \\
 b_3 &= \frac{1}{4}a_3r^3 \cosh u_0 + \frac{5}{16}a_5r^5 \\
 b_4 &= \frac{1}{8}a_4r^4u_0 \\
 b_5 &= \frac{1}{16}a_5r^5
 \end{aligned}
 \tag{32}$$

and

$$\begin{aligned}
 b'_0 &= -5a_0u_0^4 \cos u_0 + a_0u_0^5 \sin u_0 - \frac{1}{2}a_2r^2 \cos u_0 - \frac{3}{8}a_4r^4 \\
 b'_1 &= -4a_1ru_0^3 - \frac{3}{4}a_3r^3 \sinh u_0 \\
 b'_2 &= -\frac{1}{2}a_2r^2 \cos u_0 - \frac{1}{2}a_4r^4 \\
 b'_3 &= -\frac{1}{4}a_3r^3 \sinh u_0 \\
 b'_4 &= \frac{1}{8}a_4r^4
 \end{aligned}
 \tag{33}$$

The blending surface shown in Fig. 10 is obtained by setting  $a_0 = 71$ ,  $a_1 = 50$ ,  $a_2 = 2.3$ ,  $a_3 = 1.3$ ,  $a_4 = 3.8$ ,  $a_5 = 1.5$ ,  $u_0 = -0.35$  and  $u_1 = 0.35$ . Images (a) and (b) of this figure show different views of the blending surface. Despite the complexity of the primary surface, depicted in these two images, the pseudo-Lévy series method is successful in dealing with such a complex blending problem.

### 7. Conclusions

In this paper, we have developed a new method for generating blending surfaces quickly and accurately. By dividing the fourth order PDEs and their boundary conditions into two subsets, those with and without closed form solutions, the generation of a blending surface is transformed into finding the solutions of two sets of partial differential equations and their corresponding boundary conditions.

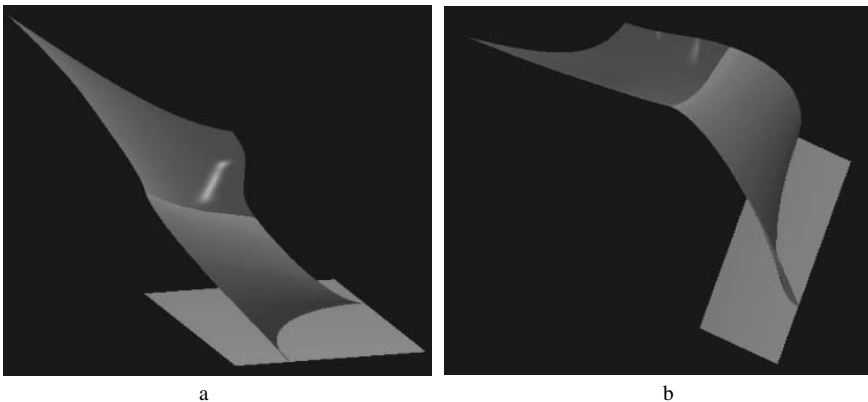


Fig. 10. The blending surface between a general surface and a plane containing a specified curve

For a PDE without a closed form solution, the functions in the boundary conditions are decomposed into a number of linearly independent basis functions. Then, the Lévy series solution of simply supported flat plates in lateral bending is modified to represent the approximate solution of the PDE. With the pseudo-Lévy series solution, the boundary conditions are satisfied exactly and the residual error of the PDE is minimised.

We have compared our method with the closed form resolution method, the Fourier series method and the pseudo-spectral method. We found that the pseudo-Lévy series method, that we have developed, can generate blending surfaces almost as fast and accurately as the closed form resolution method, more accurately and efficiently than the Fourier series method, the pseudo-spectral method and the numerical methods. In addition, our method is able to tackle complex surface modelling problems which cannot be dealt with by the closed form resolution method.

In order to demonstrate the application of our method in surface blending, we have examined the generation of blending surface between primary surfaces expressed in parametric, implicit and explicit forms.

## References

- [1] Bloor, M. I. G., Wilson, M. J.: Generating blend surfaces using partial differential equations. *Computer-Aided Design* 21(3), 165–171 (1989).
- [2] Bloor, M. I. G., Wilson, M. J.: Representing PDE surfaces in terms of B-splines. *Computer-Aided Design* 22(6), 324–331 (1990).
- [3] Cheng, S. Y., Bloor, M. I. G., Saia, A., Wilson, M. J.: Blending between quadric surfaces using partial differential equations. In: Ravani, B. (ed.): *Advances in Design Automation*, vol. 1, pp. 257–263, (1990).
- [4] You, L. H., Zhang, J. J.: Finite difference surface representation considering effect of boundary curvature. 5th International Conference on Information Visualisation, London, UK, 25–27, July, published by IEEE Computer Society, pp. 404–409, 2001.
- [5] Brown, J. M., Bloor, M. I. G., Susan, M., Wilson, M. J.: Generation and modification of non-uniform B-spline surface approximations to PDE surfaces using the finite element method. In: Ravani, B. (ed.): *Advances in Design Automation*, vol. 1, Computer Aided and Computational Design, ASME, pp. 265–272, 1990.
- [6] Brown, J. M., Bloor, M. I. G., Bloor, M. S., Wilson, M. J.: The accuracy of B-spline finite element approximations to PDE surfaces. *Computer Methods in Applied Mechanics and Engineering* 158(3–4), 221–234 (1998).
- [7] Li, Z. C.: Boundary penalty finite element methods for blending surfaces, I. Basic theory. *Journal of Computational Mathematics* 16, 457–480 (1998).
- [8] Li, Z. C.: Boundary penalty finite element methods for blending surfaces, II. Biharmonic equations. *Journal of Computational and Applied Mathematics* 110, 155–176 (1999).
- [9] Li, Z. C., Chang, C.-S.: Boundary penalty finite element methods for blending surfaces, III. Superconvergence and stability and examples. *Journal of Computational and Applied Mathematics* 110, 241–270 (1999).
- [10] Du, H., Qin, H.: Direct manipulation and interactive sculpting of PDE surfaces. *Computer Graphics Forum (EUROGRAPHICS 2000)* 19(3), 261–270 (2000).
- [11] Du, H., Qin, H.: Dynamic PDE surfaces with flexible and general geometric constraints. *Proceedings of 8th Pacific Conference on Computer Graphics and Applications*, pp. 213–222, 2000.
- [12] Du, H., Qin, H.: Integrating physics-based modeling with PDE solids for geometric design. *Proceedings of 9th Pacific Conference on Computer Graphics and Applications*, 16–18 October, Tokyo, Japan, published by IEEE Computer Society, pp. 198–207, 2001.

- [13] You, L. H., Zhang, J. J., Comninos, P.: Cloth deformation modelling using a plate bending model. The 7th International Conference in Central Europe on Computer Graphics, Visualisation and Interactive Digital Media, Plzen, Czech Republic, 8–12 February, pp. 485–491, 1999.
- [14] Bloor, M. I. G., Wilson, M. J.: Using partial differential equations to generate free-form surfaces. *Computer-Aided Design* 22(4), 202–212 (1990).
- [15] Bloor, M. I. G., Wilson, M. J.: Method for efficient parametrization of fluid membranes and vesicles. *Physical Review E* 61(4), 4218–4229 (2000).
- [16] Bloor, M. I. G., Wilson, M. J.: Spectral approximations to PDE surfaces. *Computer-Aided Design* 28(2), 145–152 (1996).
- [17] Bloor, M. I. G., Wilson, M. J.: Generating blend surfaces using a perturbation method. *Mathematical and Computer Modelling* 31(1), 1–13 (2000).
- [18] Ugail, H., Bloor, M. I. G., Wilson, M. J.: Techniques for interactive design using the PDE method. *ACM Transactions on Graphics* 18(2), 195–212 (1999).
- [19] Zhang, J. J., You, L. H.: PDE based surface representation – vase design. *Computers & Graphics* 26(1), 89–98 (2002).
- [20] Zhang, J. J., You, L. H.: Surface representation using second, fourth and mixed order partial differential equations. International Conference on Shape Modelling and Applications, Italy, 7–11 May, published by IEEE Computer Society, pp. 250–256, 2001.
- [21] Zhang, J. J., You, L. H.: Rapid generation of continuous blending surfaces. *Lecture Notes in Computer Science* 2330, 92–101 (2002).
- [22] You, L. H., Hu, J. H., Shi, Y. H., Zhang, J. J.: Single-patch surfaces for tool shape design and finite element analysis of hot metal forming. *Journal of Materials Processing Technology*, accepted for publication, 2003.
- [23] You, L. H., Zhang, J. J., Wu, H. B., Sun, R. B.: Analytical method for calculation of deformations and stresses of wall plates of dry gas holders under gas pressure. *Journal of Structural Engineering, American Society of Civil Engineers* 128(1), 125–128 (2002).
- [24] You, L. H., Zhang, J. J., Wu, H. B., Sun, R. B.: A simplified calculation method of wall plates of dry Gas holders Under gas pressure. *International Journal of Pressure Vessels and Piping* 74, 13–18 (1997).
- [25] You, L. H., Zhang, J. J., Comninos, P.: A volumetric deformable muscle model for computer animation using weighted residual method. *Computer Methods in Applied Mechanics and Engineering* 190, 853–863 (2000).

L. H. You  
Jian J. Zhang  
P. Comninos  
Bournemouth University  
Talbot Campus  
Poole  
United Kingdom  
e-mails: lyou@bournemouth.ac.uk  
jzhang@bournemouth.ac.uk  
pcomnino@bournemouth.ac.uk